Conduction mechanisms of the reverse leakage current of 4H-SiC Schottky barrier diode

Conduction mechanisms of the reverse leakage current of 4H-SiC Schottky barrier diode

A. Latreche
Département des sciences de la matière, Université de Bordj Bou Arreridj, Algeria
E-mail: hlat26@yahoo.fr

Abstract

A new numerical method for determining the reverse transition voltage between thermionic and tunneling mechanisms has been performed for 4H-SiC Schottky barrier diode. The idea of this method is based on equality between thermionic emission and tunneling process and both of them are combined with barrier lowering model. Application of this method shows a strong discrepancy between our results and that deduced from Padovani-Stratton condition. The reverse transition voltage versus the temperature plot exhibits an unexpected peak at low temperatures which means that thermionic emission mechanism predominates in this range of low temperatures. The reverse transition voltage was found increase linearly with increasing the barrier height, the effective mass and the inverse of doping concentration. In order to predict the reverse transition voltage as function of temperature, doping concentration and barrier height for 4H-SiC Schottky barrier diode an analytical model has been proposed.

Keywords: reverse transition voltage, thermionic emission, tunneling current, SiC Schottky diode, image force barrier lowering

Introduction

In recent years, the silicon carbide (4H-SiC) is promising for next generation power electronic devices because of its superior material properties and making it suitable to replace silicon in high-temperature, high-frequency and high-power applications, e.g., a 3.26 eV bandgap, a breakdown field of 3 MV/cm, about one order of magnitude larger than of silicon and a high thermal conductivity, about more than 2 times higher than that of silicon [1-4]. Theoretically, the reverse leakage current of a SiC Schottky barrier diode (SBD) significantly increases due to tunneling

process induced by the high electric fields normally encountered at the metal-semiconductor interface and it becomes larger than the thermionic emission current [5]. Also, due to the high electric fields at the metal-semiconductor interface the image force lowering of the barrier is important for SiC Schottky gates [5]. In order to describe the experimental reverse characteristics *I-V* of SiC SBDs, several authors during their analysis, used the general model [6] of the tunneling current with [7-11] and without [5] the inclusion of the image force barrier lowering (IFBL). However, several authors [12-17] showed that the thermionic field emission theory developed by Padovani-Stratton [18] can be used to describe the experimental reverse characteristics of SiC and other wide bandgap SBDs with and without the image force barrier lowering. Ivanov et *al* [19, 20] and Lee et *al* [21] concluded that the thermionic emission model combined with the barrier lowering model is appropriate to describe the reverse characteristics *I–V*. In order to describe the experimental reverse characteristics *I-V* of SiC SBDs Dolny et *al* [22] proposed a model based on a combination of trap-assisted tunneling and a thermionic-emission mechanism through a potential barrier located at the metal-SiC interface.

Zheng et *al* [23] analyzed the reverse characteristics of 6H-SiC SBD at 300 K by a treatment that includes the effect of barrier height fluctuations and image charge lowering on both the thermionic emission and electron tunneling processes by using WKB (Wentzel–Kramers–Brillouin) approximation. They found a very good agreement with published experimental data at 300 K. In their study the reverse transition voltage between the thermionic emission and tunneling mechanisms was about 265 V. The condition which gives the minimum reverse bias to apply to the diode in order to observe thermionic-field emission is given analytically by Padovani-Stratton [18]. Note that the theory of Padovani-Stratton [18] is an approximation of the general tunneling model and it does not include the image force effect. Hatakeyama and Shinohe [24] identified numerically the dominant mechanisms of the reverse leakage current of 4H-SiC SBD as a function of the electric field and Schottky barrier height from the field emission, thermionic field emission and the

barrier lowering models at 300 K. These all studies have been performed for low reverse bias or for high reverse bias.

In this paper, we investigate a numerical study in order to identify which mechanism is dominant in 4H-SiC Schottky barrier diode when a reverse bias voltage is applied to the junction for a given temperature range. The influence of several parameters is investigated such as; barrier height, doping concentration and effective mass. The idea of this study is based on equality between thermionic emission and tunneling process and both of them are combined with barrier lowering model.

Theory

The dominant mechanisms by which carrier transport occurs in Schottky barriers are thermionic emission over the potential barrier and carrier tunneling through the potential barrier [25]. The total electron current density flowing through the Schottky potential barrier is calculated according to the Tsu–Esaki formalism [6, 9, 26, 27]

$$J_{Tun} = \frac{A^* T}{k_B} \int_0^\infty T\left(E_x\right) \ln\left(\frac{1+\exp\left(-q\zeta - E_x\right)/k_B T}{1+\exp\left(-q\zeta - qV_R - E_x\right)/k_B T}\right) dE_x \quad (1)$$

Where k_B *is* the Boltzmann constant, T is the temperature, A^* is the effective Richardson constant, ζ denotes a difference between the equilibrium Fermi level and conduction bands and $T\left(E_x\right)$ is the tunneling probability. In our calculations we use the *WKB* approximation to calculate the tunneling probability $T\left(E_x\right)$.

$$T_{WKB}\left(E_x\right) = \exp\left[-2\int_{x_1}^{x_2}\left(\frac{2m^*}{\hbar^2}\left(U(x) - E_x\right)\right)^{1/2} dx\right] \quad (2)$$

where, x_1 and x_2 are the two turning points. The WKB can predict tunneling current through a Schottky barrier with reasonable accuracy [28]. Including the effect of the force barrier lowering, the potential energy, $U(x)$, of the barrier as measured with respect to the energy of the bottom of the conduction band in the bulk of the material is given by [9, 23]

$$U(x) = \frac{q^2 N_D}{2\varepsilon_S}(D - x)^2 - \frac{q^2}{16\pi\varepsilon_S x} \tag{3}$$

Where N_D is the doping density, D is the depletion width, dependent on the reverse bias voltage V_R, ε_S is the semiconductor permittivity.

In the current equation (1) the both mechanisms of the conduction carriers flow in SBD are included: thermionic emission occurs for energy higher than the maximum of the potential Schottky barrier ($E_x > U_{max}$), and tunneling process occurs for the lower energy range ($E_x < U_{max}$) [9, 27].

$$J_{Tot} = J_{Tun} + J_{Therm} \tag{4}$$

Where the reverse tunneling current density is given by [6, 9, 26, 27]

$$J_{Tun} = \frac{A^* T}{k_B} \int_0^{U_{max}} T(E_x) \ln\left(\frac{1+\exp(-q\zeta - E_x)/k_B T}{1+\exp(-q\zeta - qV_R - E_x)/k_B T}\right) dE_x \tag{5}$$

And the thermionic emission current density with including the image force lowering is expressed by [9, 27]:

$$J_{Therm} = \frac{A^* T}{k_B} \int_{U_{max}}^{\infty} T(E_x) \ln\left(\frac{1+\exp(-q\zeta - E_x)/k_B T}{1+\exp(-q\zeta - qV_R - E_x)/k_B T}\right) dE_x \tag{6}$$

By setting the tunneling probability $T(E_x)$=1 for the energies higher than the maximum of the Schottky potential barrier and by approximating the Fermi–Dirac statistics with the Maxwell–Boltzmann one, the equation (6) of the thermionic emission current with including the effect of image force lowering can be re-write as [9, 27]

$$J_{Therm} = A^* T^2 e^{-\frac{q}{k_B T}(\phi_b - \Delta\phi_b)}\left(e^{\frac{qV}{k_B T}} - 1\right) \tag{7}$$

Where the image force lowering is given by [29]:

$$\Delta\phi_b = \left[\frac{q^3 N_D (\phi_b - \zeta - V_R)}{8\pi^2 \varepsilon_s^3}\right]^{1/4} \tag{8}$$

Starting from the general expression of the tunneling current given by equation (5), Padovani and Stratton [18] developed the theory of field emission (FE) and thermionic field emission (TFE) by assuming a simple parabolic shape (image force lowering was neglected) and by employing a WKB

tunneling probability approximation. In the intermediate temperature range, the thermionic field emission is dominated; while the current is dominated by pure field emission when the temperature gets lower or the reverse bias gets higher [18].

Padovani and Stratton [18] derived their model by taking only the first two terms of the Taylor series expansion of the exponent of the transparency of the barrier around the Fermi level for field emission model and the first three terms of the Taylor series expansion around energy E_m above the bottom of the conduction band for thermionic field emission model, and therefore has restrictions that must be met to ensure accuracy. The currents density due to TFE and FE are given by [18]

$$J_{TFE} = \frac{A^* T}{k_B}\sqrt{\pi E_{00} q\left(-V + \frac{\phi_b}{\cosh^2\left(E_{00}/k_B T\right)}\right)}\exp\left(-\frac{q\phi_b}{E_0}\right)\exp\left(-\frac{qV}{\varepsilon'}\right) \tag{9}$$

$$J_{FE} = \frac{A^* T^2 \pi E_{00}\exp\left[-2q\phi_b^{3/2}/3E_{00}\left(\phi_b - V\right)^{1/2}\right]}{k_B T\left[\phi_b/\left(\phi_b - V\right)\right]^{1/2}\sin\left\{\pi k_B T\left[\phi_b/\left(\phi_b - V\right)\right]^{1/2}/E_{00}\right\}} \tag{10}$$

Where

$$\varepsilon' = \frac{E_{00}}{\left(E_{00}/k_B T\right) - \tanh\left(E_{00}/k_B T\right)} \tag{11}$$

$$E_0 = E_{00}\coth\left(E_{00}/k_B T\right) \tag{12}$$

$$E_{00} = \frac{h}{4\pi}\left(\frac{N_D}{m^* \varepsilon_s}\right) \tag{13}$$

The minimum voltage to be applied for thermionic-field emission is [18]

$$-V > \phi_b + \frac{3E_{00}}{2q}\frac{\cosh^2\left(E_{00}/k_B T\right)}{\sinh^3\left(E_{00}/k_B T\right)} \tag{14}$$

The condition which gives the transition between thermionic field emission (TFE) and field emission (FE) is given by a constant $c_1\left(c_1 = E_{00}^{-1}\left[\phi_b/\left(\phi_b - V\right)\right]^{1/2}\right)$ where

$$\begin{cases} 1/c_1 < k_B T, & For \quad TFE \\ 1/c_1 > k_B T, & For \quad FE \end{cases} \tag{15}$$

Results and discussion

Simulation of reverse characteristics *I-V* of 4H-SiC Schottky diode is performed by the effective Richardson constant A^* = 146 A K^{-1} cm^{-2}, the effective mass $m^* = 0.2m_0$ [30, 31] and $\phi_b = 1eV$.

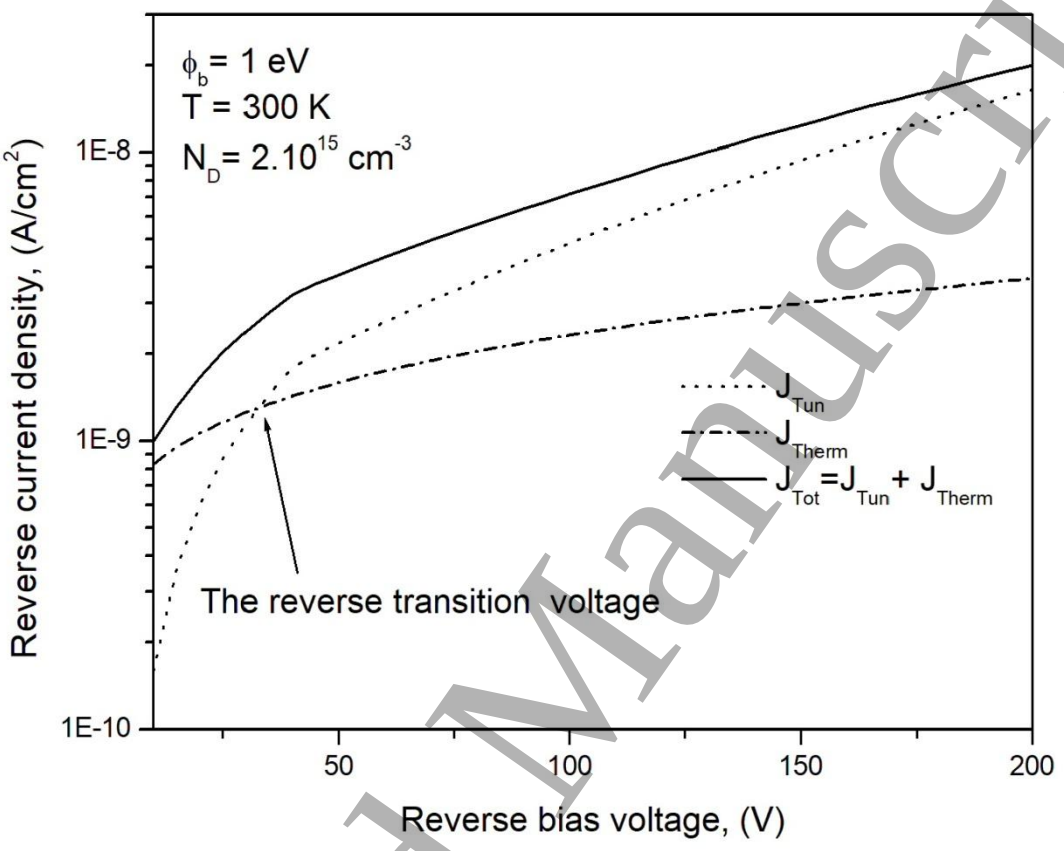

Figure 1. Reverse current–voltage characteristics based on both the thermionic emission and tunneling processes for 4H-SiC SBD with including the image force lowering.

Figure 1 shows the calculated reverse current densities with the image force barrier lowering according to tunneling and thermionic models for 4H-SiC Schottky diode at room temperature with doping concentration N_D = 2.10^{15} cm^{-3}, barrier height $\phi_b = 1eV$ and effective mass $m^* = 0.2m_0$. The total current is the sum of both components. The reverse transition voltage (V_T) between thermionic emission and tunneling currents represents the value of the intersection of the both curves *I-V* which can be obtained numerically by solving the equation $J_{tun} = J_{therm}$ or directly from the intersection between the generated curves *I-V* as shown in figure 1. The transition between

thermionic emission and tunneling occurs at approximately V_T = 32 V reverse bias. At low voltages (V << 32 volts) the thermionic emission component is seem to be dominant, while the tunneling mechanism becomes larger for high voltages (V >> 32 volts). Near the reverse transition voltage, neither tunneling nor thermionic emission accurately describes the conduction process because the both currents have the same order of magnitude, therefore the both mechanisms must be combined together.

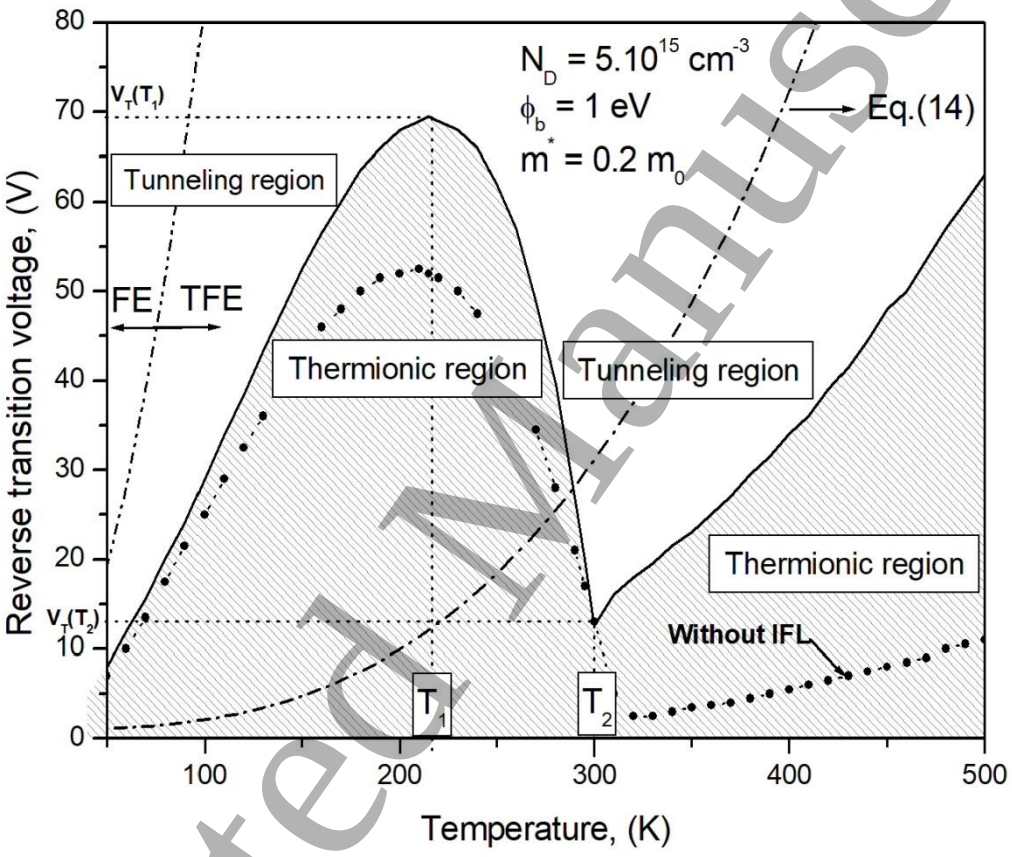

Figure 2. Reverse transition voltage versus temperature plots and showing the regions of thermionic and tunneling in the case when the image force lowering is included. Comparison with Padovani-Stratton's condition.

In order to obtain the reverse transition voltage versus the temperature plot we must generate the reverse characteristics based on both the thermionic emission and tunneling process for each temperature and determine the reverse transition voltage directly from the intersection between the generated curves *I-V-T* as we did in the precedent paragraph for T = 300 K. The obtained values of

the reverse transition voltage for each temperature are plotted in Figure 2 for doping concentration N_D =5 .10^{15} cm^{-3}, barrier height $\phi_b = 1eV$ and effective mass $m^* = 0.2m_0$. For comparison we show also the reverse transition voltage without image force lowering by using our method (equations 3, 5 and 7 without image force lowering) and by using the Padovani-Stratton's condition given by equation (14). It is clear from this figure that for low (< 220 K) and high (> 300 K) temperatures the reverse transition voltage increases with increasing temperature, however, for intermediate temperatures (220-300 K) the reverse transition voltage decreases with increasing temperature. This behavior makes in the curve, first a relative maximum point at approximately T_1 = 220 K followed by a relative minimum point at approximately T_2 = 300 K. Above the curve of reverse transition voltage versus temperature the tunneling current is larger than the thermionic current and below it the thermionic current is larger than tunneling current. Around the low temperature T_1 which corresponds to the relative maximum point, the thermionic emission mechanism is preponderant across a bit high range of reverse bias.

The delimited regions of thermionic and tunneling is the result of the competition between the both mechanisms; thermionic and tunneling when we change the values of temperature and reverse bias simultaneously. The increase in the temperature leads to an increase in the both components, each one of them increased by a certain amount according to the value of the reverse bias. It is the same when the reverse bias is increased; it leads to an increase in the both components by a certain amount according to the value of temperature. The increase in reverse bias causes the potential barrier to become thin enough for electrons in the metal to tunnel into the semiconductor at energies below the top of the barrier and the increase of the thermionic emission is due to the reduce of the barrier height by effect of the image force lowering. When the reverse bias is increased, the amount of the increase in thermionic emission is less compared with the amount of the increase in tunneling. In the delimited region where the temperature is less than T_1 the reverse transition voltage is increased which means that the amount of the increase in thermionic emission component due to the increase in temperature is larger than the tunneling component, and in order for the two

components to be equal, the tunneling component should be increased by increasing the reverse bias voltage. In the region where the temperature is greater than T_1 and less than T_2 we have the opposite situation; the amount of the increase in tunneling component due to the increase in temperature becomes larger than the thermionic emission component, hence, in order for the two components to be equal, the tunneling component should be reduced by decreasing the reverse bias voltage. Beyond the temperature T_2 the process will inversed again, and the amount of the increase in thermionic emission component becomes larger than the tunneling component but in the same order of magnitude with tunneling component, so, in order for the two components to be equal, the tunneling component should be increased by increasing the reverse bias voltage by a small amount compared with the two first regions which exhibit a strong slop. When the image force lowering is ignored, we get the same behavior with a less reverse transition voltage because the amount of the increase (or decrease) in thermionic emission current due to the image force lowering caused by increase (or decrease) in the reverse bias is omitted. The phenomenon described above is unexpected by the Padovani-Stratton model that expects an increase of reverse transition voltage with increasing temperature as shown in figure 2. This discrepancy between our result and Padovan-Stratton's condition is mainly due to the approximation occurred at the level of the transparency in the Padovan-Stratton's model.

If the reverse transition voltage is fixed between the two reverse transition voltages V_T (T_1) and $V_T(T_2)$ which correspond to relative maximum and minimum points, respectively, the increase of the temperature from the lower temperatures to higher temperatures makes a competition between the tunneling and thermionic mechanisms as shown in figure3. Increasing the temperature from lower temperatures, the dominant process is the tunneling mechanism till the first intersection point between the both curves *I-V*. Above of this first intersection point the thermionic mechanism becomes the dominant process. Increasing again the temperature the curves of the both currents intersect again in second point and the tunneling mechanism becomes small larger than the thermionic mechanism. Increasing again the temperature the two curves of the current intersect in

the third point, and above of this point the thermionic current will maintain the dominant mechanism and it is in the same order of magnitude with tunneling current.

If the voltage is located above of the V_T (T_1) which corresponds to the relative maximum point, the dominant mechanism from the lower temperatures to the higher temperatures is tunneling process. At very high temperatures the thermionic current becomes small larger than the tunneling current and both of them are in the same order of magnitude. In contrast, if the voltage is below the transition voltage V_T (T_2) which corresponds to the relative minimum point, the dominant mechanism at very lower temperatures is tunneling process then the thermionic mechanism will become the dominant process from the low temperatures until the higher temperatures. Above the temperature T_2 the tunneling current will become in the same order of magnitude with thermionic current.

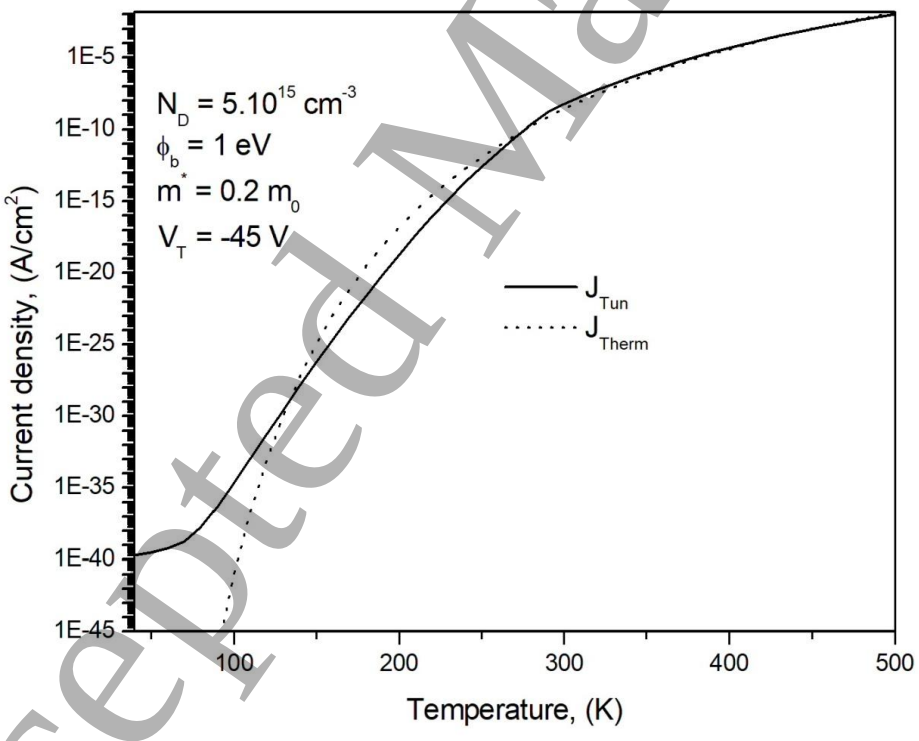

Figure 3. Thermionic and tunneling current densities as a function of temperature for 4H-SiC SBD at reverse voltage of 45 V. The image force lowering is included.

The influence of the doping concentration on the reverse transition voltage is shown in figure 4. The reverse transition voltage decreases with increasing the doping concentration due to the increase of the tunneling probability because the electrons see a thinner barrier. The tow temperatures T_1 and T_2 where the relative maximum and minimum occur respectively do not change when the doping concentration is varied. For a fixed temperature the reverse transition voltage increases linearly with the inverse of doping concentration (N_D^{-1}) as shown in figure 5.

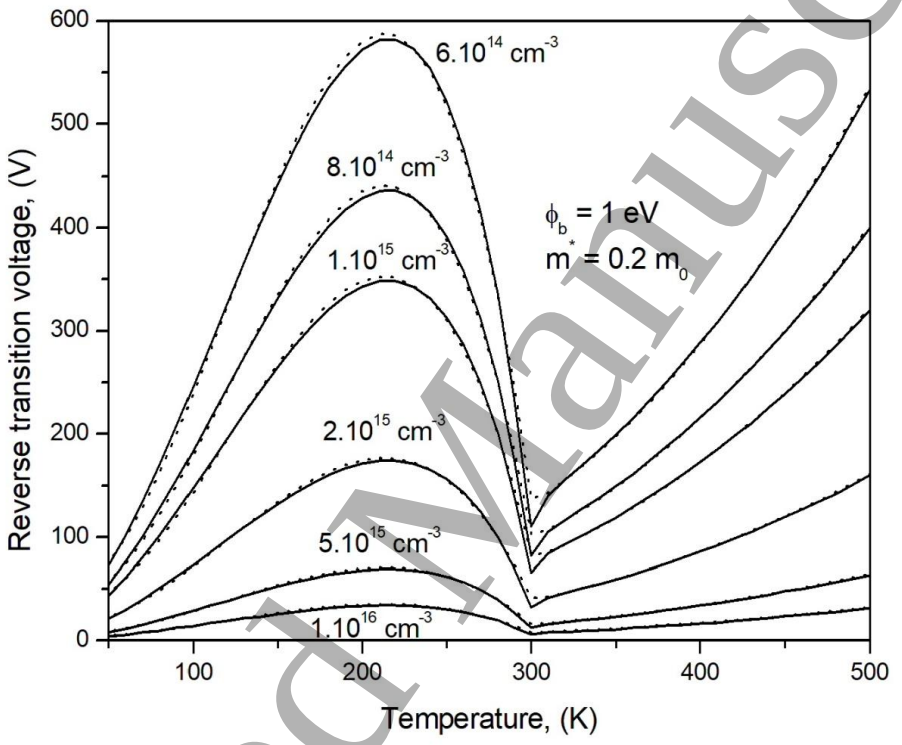

Figure 4. Reverse transition voltage versus temperature plot for various doping concentrations for 4H-SiC SBD. The dotted lines are the curves fitted by using our proposed model (equations (16) and (17)).

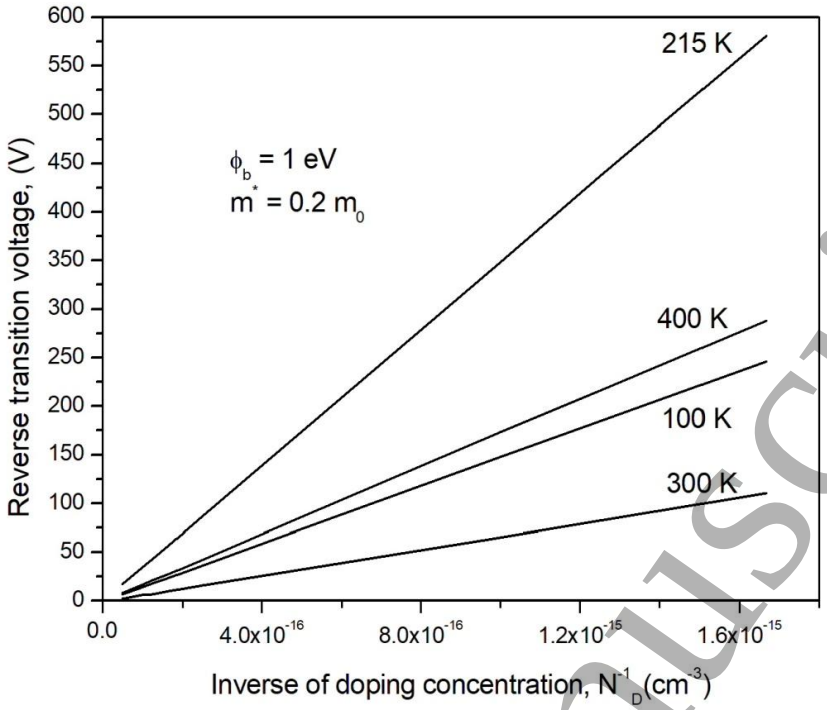

Figure 5. Reverse transition voltage as a function of the inverse doping concentration for various temperatures for 4H-SiC SBD.

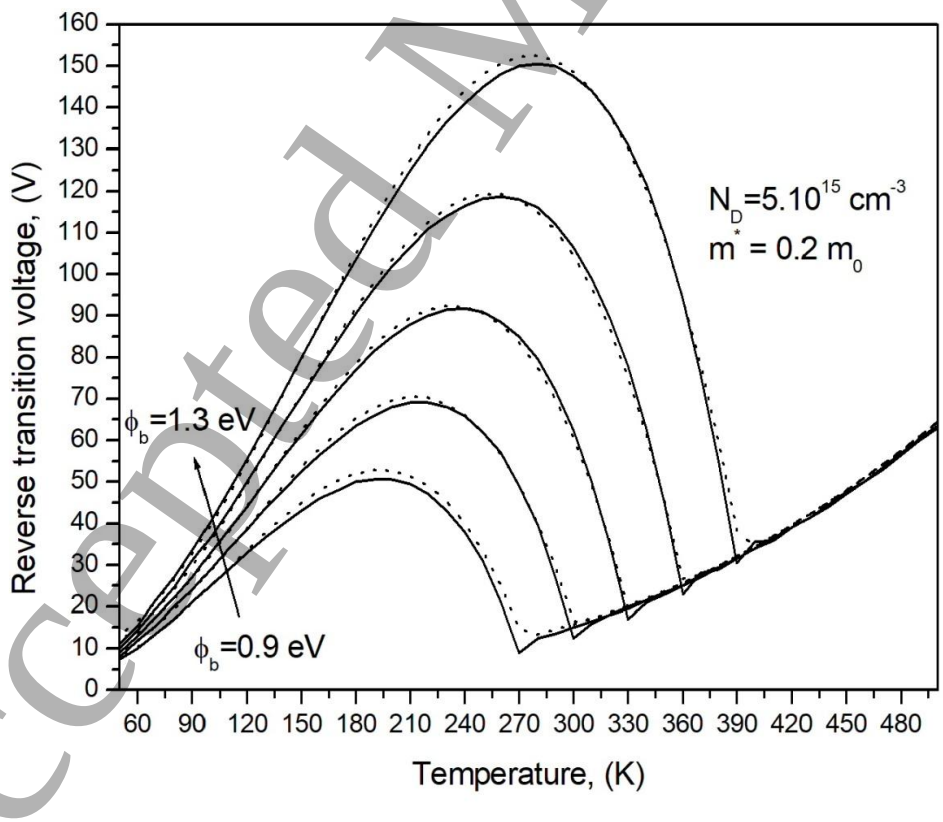

Figure 6. Reverse transition voltage versus temperature plot for various barrier heights for 4H-SiC SBD. The dotted lines are the curves fitted by using our proposed model (equations (16) and (17)).

Reverse transition voltage as a function of temperature is shown in figure 6 for various barrier heights for 4H-SiC SBD. The tow temperatures of the two relative extremes T_1 and T_2 increase linearly when the barrier height increases according to the following equations: $T_1 = 20 + 200\phi_b$ for T_1 and $T_2 = 300\phi_b$ for T_2. For a fixed temperature (T^*), which in turn represents a temperature of the relative minimum (T_2^*) corresponding to the any barrier height (ϕ_b^*) (for example, T_2^* = 300 K corresponds to the barrier height ϕ_b^* = 1 eV as shown in figure 6), the reverse transition voltage remains constant for the barrier heights that below of ϕ_b^*, beyond the barrier height ϕ_b^*, the reverse transition voltage starts to increase linearly with increasing the barrier height as shown in figure 7 for various temperatures 270-390 K with the step of 30 K.

The variation of the reverse transition voltage versus the barrier height is due to the decrease of both components of the current by the same value as a function of barrier height till the barrier height which corresponds to the temperature of the relative minimum T_2 where the tunneling current decreases faster than the thermionic current as shown in the inset graph in figure7 .

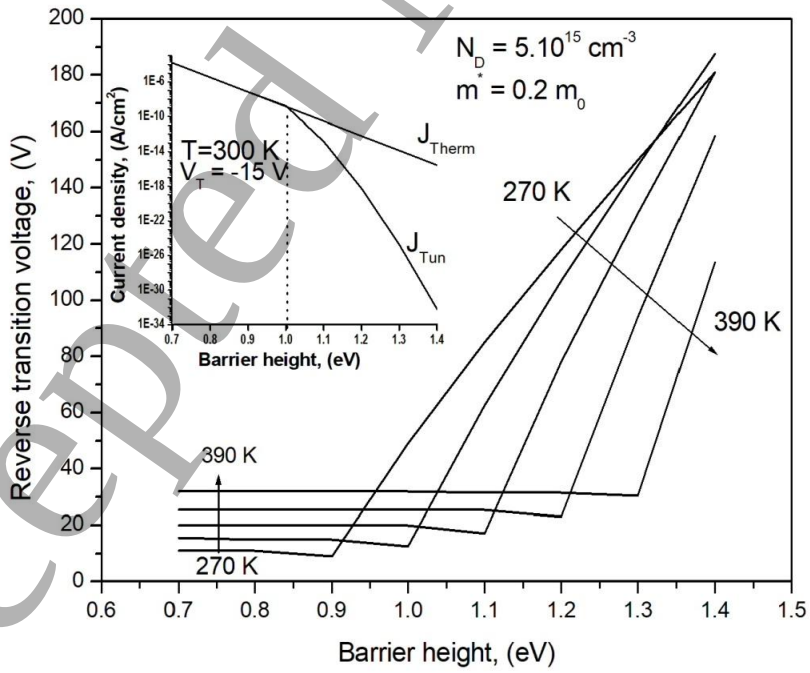

Figure 7. Reverse transition voltage as a function of barrier height for various temperatures for 4H-SiC SBD. The inset shows the current densities J_{Tun} and J_{Therm} versus barrier height at 300 K and V_T = -15 Volts.

The evolution of the reverse transition voltage as a function of the temperature at different effective mass is plotted in figure 8. It is clear from this figure that the temperature T_1 which corresponds to the relative maximum does not vary with variation of the effective mass, while the temperature T_2 which corresponds to the relative minimum decreases slightly when the effective mass increases. For a fixed temperature the reverse transition voltage increases linearly with increasing the effective mass as shown in the figure 9. The increase in the reverse transition voltage as a function of effective mass is due to decrease in tunneling current more than the thermionic emission.

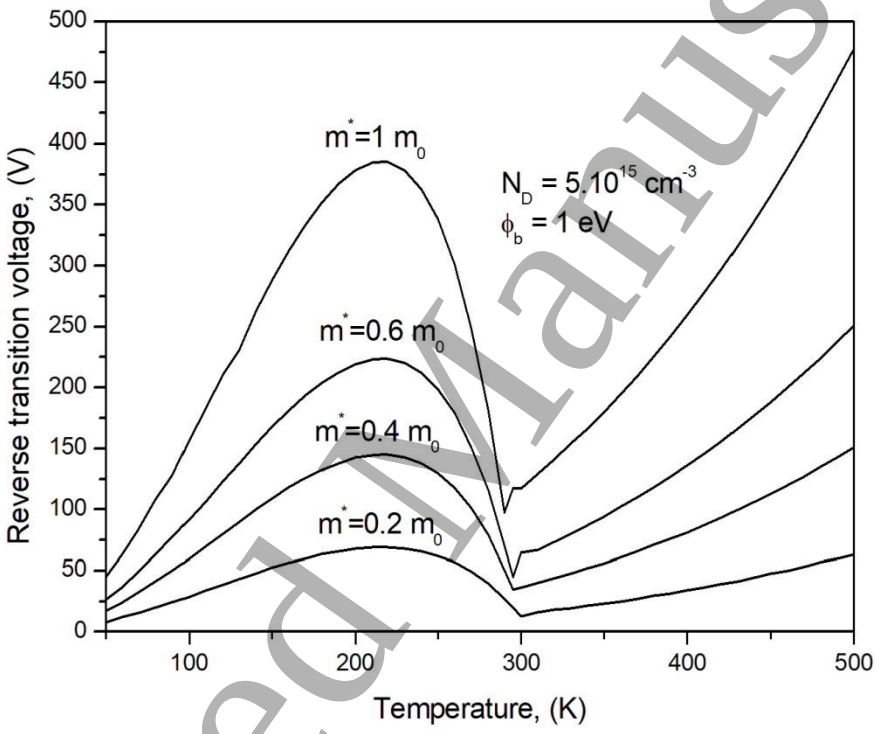

Figure 8. Reverse transition voltage versus temperature plot for various effective mass for 4H-SiC SBD.

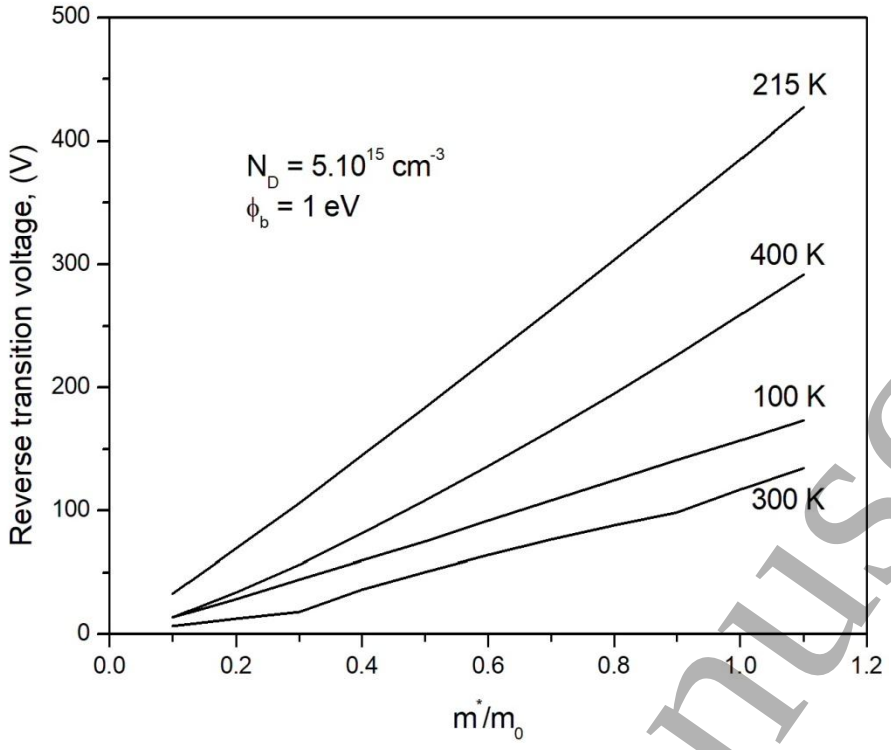

Figure 9. Reverse transition voltage as a function of effective mass for various temperatures for 4H-SiC SBD.

In order to increase the reverse transition voltage, in other words, decrease the reverse tunneling current; we must use semiconductors which have a large band gap and high effective mass.

The reverse transition voltage versus the temperature plot has a complicated shape, so, the fit of the data with an analytical function is very difficult. Thus, we propose to fit the data with two simple analytical functions over tow ranges of temperature. The first range is started from the lower temperatures (The temperatures less than 50 K were omitted since for low temperatures, the currents are very small, difficult to calculated, and of little interest) up to the temperature T_2 which corresponds to the relative minimum point and linearly depends on barrier height according to this equation $T_2 = 300\phi_b$. We found that the simplest and most appropriate analytical function for fitting the data in this range of temperature is the third degree polynomial with four coefficients. By varying the barrier height and fitting the corresponding data we found that each coefficient of the third degree polynomial is a straight line. The second range of temperature begins from T_2 up to

higher temperatures. In this range of temperature we found that the simplest and most appropriate analytical function is the second degree polynomial (parabola). As we found above this function is independent of barrier height in this range of temperature (see figure 6). Then, by using the result that the reverse transition voltage linearly depends on the inverse of doping concentration we can rearrange the tow obtained functions by multiplying them by $1/N_D$. The following function relationships can be obtained for 4H-SiC SBD:

$$V_T \approx \begin{cases} \left[f(\phi_b) + g(\phi_b)T + h(\phi_b)T^2 + p(\phi_b)T^3\right]\dfrac{10^{15}}{N_D} & for\ 50\,K \le T \le T_2 = 300\phi_b \\ \left[137.301 - 1.04T + 2.8210^{-3}T^2\right]\dfrac{10^{15}}{N_D} & for\ T \succ T_2 = 300\phi_b \end{cases} \quad (16)$$

Where the functions $f(\phi_b)$, $g(\phi_b)$, $h(\phi_b)$ and $p(\phi_b)$ are linearly dependent on the barrier height and given by

$$\begin{cases} f(\phi_b) = -39.027 + 85.179\phi_b \\ g(\phi_b) = 6.13410^{-2} - 1.548\phi_b \\ h(\phi_b) = (11.124 + 23.13\phi_b)10^{-3} \\ p(\phi_b) = (-114.836 + 18.5\phi_b)10^{-6} \end{cases} \quad (17)$$

The equations (16) and (17) are obtained by using the parameters: A^*= 146 A K^{-1} cm^{-2}, $m^* = 0.2m_0$ and $\varepsilon_S = 10\varepsilon_0$. From the equations (16) and (17) we can predict the reverse transition voltage between the thermionic and tunneling mechanisms for any temperature range and reverse bias range; therefore we can choose the appropriate conduction mechanisms for analysis the experimental data of 4H-SiC SBDs. As shown in figures (4) and (6), our proposed analytical model which is indicated by dotted lines is in good agreement with the simulated data.

Conclusion

The dominant mechanisms of the reverse leakage current of the Schottky barrier diode are determined as a function of reverse bias voltage and temperature from the general expression of the tunneling current and thermionic emission model. Both of the mechanisms are combined with the barrier lowering model. The calculated results show that the thermionic emission current dominates

the reverse leakage current of 4H-SiC Schottky diode at low temperatures over a bit high range of reverse bias voltage. The reverse transition voltage between thermionic emission and tunneling process is strongly depends on the temperature, barrier height, doping concentration and effective mass. A simple analytical model has been proposed for calculating the reverse transition voltage as a function of temperature, doping concentration and barrier height.

References

[1] Mahajan A and Skromme B J 2005 Design and optimization of junction termination extension (JTE) for 4H-SiC high voltage Schottky diodes *Solid-State Electron.***49** 945-55
[2] Matsunami H 2006 Current SiC technology for power electronic devices beyond Si *Microelectron. Eng.* **83** 2-4
[3]Kimoto T 2015 Material science and device physics in SiC technology for high-voltage power devices *Jpn. J. Appl. Phys.* **54** 040103
[4] Privitera S M S, Litrico G, Camarda M, Piluso N, and Francesco La Via F 2017 Electrical properties of extended defects in 4H-SiC investigated by photoinduced current measurements *Appl. Phys. Express* **10** 036601
[5] Crofton J and Sriram S 1996 Reverse Leakage Current Calculations for SiC Schottky Contacts *IEEE Trans.Electron. Devices* **43** 2305-7
[6] Tsu R and Esaki L 1973 Tunneling in a finite superlattice *Appl. Phys. Lett.* **22** 562-4
[7] Eriksson J, Rorsman N and Zirath H 2003 4H-Silicon Carbide Schottky Barrier Diodes for Microwave Applications *IEEE Trans.Microwave Theory Technol.* **51** 796-804
[8] Blasciuc-Dimitriu D, Horsfall A B, Wright N G, Johnson C M, Vassilevski K V and O'Neill A G 2005 Quantum modelling of I–V characteristics for 4H–SiC Schottky barrier diodes Semicond.Sci.Technol. **20** 10-5
[9] Furno M, Bonani F and Ghione G2007 Transfer matrix method modelling of inhomogeneous Schottky barrier diodes on silicon carbide *Solid-State Electron.***51** 466-74
[10] Latreche A 2014 Reverse bias-dependence of schottky barrier height on silicon carbide: influence of the temperature and donor concentration *Int. J .Phys. Res.* **2** 40-9
[11] Okino H, Kameshiro N, Konishi K, Shima A and Yamada R 2017 Analysis of high reverse currents of 4H-SiC Schottky-barrier diodes *J. Appl. Phys.* **122**, 235704
[12] Treu M, Rupp R, Kpels H and Bartsch W 2001 Temperature Dependence of Forward and Reverse Characteristics of Ti, W, Ta and Ni Schottky Diodes on 4H-SiC *Materials Science Forum* **353-356** 679-82
[13] Oyama S, Hashizume T and Hasegawa H 2002 Mechanism of Current Leakage through Metal/n-GaN interfaces *Appl.Surf. Sci.***190** 322-5
[14] Hatakeyama T, Kushibe M, Watanabe T, Imai S and Shinohe T 2003 Optimum Design of a SiC Schottky Barrier Diode Considering Reverse Leakage Current due to Tunneling Process Mat. Sci. Forum **433-436** 831-4
[15] Xie K, Hartz S A, Ayres V M, Jacobs B W, Ronningen R M, Zeller A F, Baumann T and Tupta M A 2015 Thermionic field emission in GaN nanoFET Schottky barriers *Mater. Res. Express* **2** 015003
[16] Kim H 2016 Reverse-bias Leakage Current Mechanisms in Cu/n-type Schottky Junction Using Oxygen Plasma Treatment *Trans. Electr. Electron. Mater.* **17** 113-7
[17] Higashiwaki M et *al* 2016 Temperature-dependent capacitance–voltage and current–voltage characteristics of Pt/Ga_2O_3 (001) Schottky barrier diodes fabricated on n–Ga_2O_3 drift layers grown by halide vapor phase epitaxy *Appl. Phys. Lett.* **108** 133503

[18] Padovani F A and Stratton R 1962 Field and thermionic-field emission in Schottky barriers Solid-State Electron. **9** 695-707
[19] Ivanov P A, Grekhov I V, Kon'kov O I, Potapov A S, Samsonova T P, and Semenov T V 2011 *I–V* Characteristics of High-Voltage 4*H*–SiC Diodes with a 1.1-eV Schottky Barrier *Semiconductors* **45** 1374–77
[20] Ivanov P A, Grekhov I V, Potapov A S , Il'inskaya N D, Kon'kov O I, Samsonova T P 2013 Reverse Leakage Currents in High-Voltage 4H-SiC Schottky Diodes *Materials Science Forum* **740-742** 877-80
[21] Lee K Y, Liu Y H, Wang S C, Chan L S 2017 Influence of the Design of Square p+ Islands on the Characteristics of 4H-SiC JBS *IEEE Trans.Electron. Devices* **64** 1394-8
[22] Dolny G, Sheng Y, Fu Y, Li S, Radharkrishnan R, Woodin R L 2018 Multi-Level Trap Assisted Tunneling Model for the Field and Temperature Dependence of SiC-JBS Reverse Leakage Current *Materials Science Forum* **924** 601-4
[23] Zheng L, Joshi R P and Fazi C 1999 Effects of barrier height fluctuations and electron tunneling on the reverse characteristics of 6H–SiC Schottky contacts *J. Appl. Phys.* **85** 3701-7
[24] Hatakenama T and Shinohe T 2002 Reverse characteristics of a 4H-SiC Schottky barrier diode *Materials Science Forum* **389-393** 1169-72
[25] Rhoderick E H 1982 Metal-semiconductor contacts *IEE PROC*, **129** 1-14
[26] Eriksson J, Rorsman N and Zirath H 2003 4H-Silicon Carbide Schottky Barrier Diodes for Microwave Applications *IEEE Trans.Microwave Theory Technol.* **51** 796-804
[27] Huang L 2016 Barrier inhomogeneities of platinum contacts to 4H-SiC *Superlattices and Microstructures* **100** 648-55
[28] Latreche A and Ouennoughi Z 2013 Modified Airy function method modeling of tunnelling current for Schottky barrier diodes on silicon carbide Semicond. Sci. Technol. **28** 105003(8pp)
[29] Rhoderick E H and Williams R H 1988 *Metal–Semiconductor Contact* (Oxford: Oxford University Press) for example
[30] Itoh A and Matsunami H 1997 Analysis of Schottky Barrier Heights of Metal/SiC Contacts and Its Possible Application to High-Voltage Rectifying Devices*Phys. Status Solidi a* **162** 389-408
[31] Roccaforte F 2003 Richardson's constant in inhomogeneous silicon carbide Schottky contacts *J. Appl. Phys.* **93** 9137- 44